Materials Research, Vol. 11, No. 1, 17-21, 2008

Microstructure and Composition of Rare Earth-Transition Metal-Aluminium-Magnesium Alloys

*Lia Maria Carlotti Zarpelon, Eguiberto Galego, Hidetoshi Takiishi, Rubens Nunes Faria**

Instituto de Pesquisas Energéticas e Nucleares – IPEN,
Av. Prof. Lineu Prestes, 2242, Cidade Universitária, 05508900 São Paulo - SP, Brazil

Received: February 8, 2007; Revised: January 22, 2008

The determination of the microstructure and chemical composition of $La_{0.7-x}Pr_xMg_{0.3}Al_{0.3}Mn_{0.4}Co_{0.5}Ni_{3.8}$ ($0 \leq x \leq 0.7$) metal hydride alloys has been carried out using scanning electron microscopy (SEM), energy dispersive X ray analysis (EDX) and X ray diffraction analysis (XRD). The substitution of La with Pr changed the grain structure from equiaxial to columnar. The relative atomic ratio of rare earth to (Al, Mn, Co, Ni) in the matrix phase was 1:5 ($LaNi_5$-type structure). Magnesium was detected only in two other phases present. A grey phase revealed 11 at.% Mg and the concentration ratios of other elements indicated the composition to be close to $PrMgNi_4$. A dark phase was very heterogeneous in composition, attributed to the as-cast state of these alloys. The phases identified by XRD analysis in the $La_{0.7}Mg_{0.3}Al_{0.3}Mn_{0.4}Co_{0.5}Ni_{3.8}$ alloy were: $La(Ni,Co)_5$, $LaAl(Ni,Co)_4$, $La_2(Ni,Co)_7$ and $AlMn(Ni,Co)_2$. Praseodymium favors the formation of a phase with a $PuNi_3$-type structure. Cobalt substituted Ni in the structures and yielded phases of the type: $Pr(Ni,Co)_5$ and $Pr(Ni,Co)_3$.

Keywords: *rare earth, transition metal, microanalyses, XRD, EDX*

1. Introduction

Since the development of $LaNi_5$-based hydrogen storage alloys, there have been many studies related to substitutions of various alloying elements in the basic composition. Substitution of alloying elements in La-Ni-type electrodes and their effects have been widely reported. The purpose of alloy modification is to improve electrode performance, i.e., high hydrogen storage capacity, improve kinetics of hydrogen absorption and desorption, increase cycle life, improve corrosion resistance, etc. In the past a small amount of praseodymium was added to these materials, along with mish metal (MM)[1-10]. Optimization of the Pr content (from 0 to 0.4 at.% in the alloy) with respect to electrochemical properties of $MMAl_{0.3}Mn_{0.3}Co_{0.4}Ni_{4.0}$ alloys (MM = LaNdPr) has also been reported[11]. It has been shown that the electrochemical properties of the electrode made with the alloy containing about 20 at.% Pr in the MM were significantly improved. The electrode prepared from this alloy had a higher capacity, better discharge rate characteristics and longer cycle life than that prepared from an alloy with less than 10 at.% Pr in the MM. AA size cells in which the $(LaNdPr)Al_{0.3}Mn_{0.4}Co_{0.8}Ni_{3.5}$ electrode alloy contained about 17 at.% Pr in the MM showed a very long cycle life (1400 cycles) with reasonable capacity (1250 mAh) and also discharged rate capacity (1100 mAh at 5 C)[11]. These batteries also showed higher capacity at low temperatures (1050 mAh when discharged at 1 °C and –18 °C). Recently, it has been shown that a $PrMg_2Ni_9$ alloy has good cycle life and an amorphous $PrMgNi_4$ alloy, good discharge capacity[12]. A systematic investigation of complete substitution of La with Pr in Mg-containing hydrogen storage alloys (Nd-free) has not yet been reported. There are few reports about the microstructures and composition of the phases in these alloys. This paper addresses this aspect and reports the results of a systematic study of hydrogen storage alloys of the type $La_{0.7-x}Pr_xMg_{0.3}Al_{0.3}Mn_{0.4}Co_{0.5}Ni_{3.8}$ ($x = 0, 0.1, 0.3, 0.5$ and 0.7). A thorough investigation of the microstructures of these alloys and the phases present there in has been carried out using SEM (+EDX) and XRD. This is a necessary stage, prior to production of negative electrodes for batteries using alloys based on these compositions.

*e-mail: rfaria@ipen.br

2. Experimental

Various commercial alloys in the as-cast state were studied in this investigation. The chemical analyses of the as-cast alloys are given in Table 1. For convenience of comparison, the equivalent substituted composition, in at.%, is also given. Good agreement was found between the specified composition values and those determined by analyses of the alloys. As per the supplier's specification, the alloys contained sulfur, oxygen and nitrogen as impurities (<10 ppm). Samples for microstructure studies were prepared using conventional metallographic procedures. The microstructures of the specimens were examined using a scanning electron microscope with an energy dispersive X ray analysis facility. Average data were obtained from separate measurements carried out on the different phases. Powder samples of the alloys (<125 μm) were analyzed using the X ray diffraction (XRD) technique, with Cu K_α radiation. Identification of the various phases was carried out by comparison with standards in the ICDD data base and using the software "Crystallographica Search-Match" (CSM).

3. Results and Discussion

Backscattered electron micrographs of as-cast alloys containing lanthanum or praseodymium (x = 0 and 0.7) are shown in Figures 1 and 2, respectively. The former shows a typical equiaxial grain structure, whereas the latter reveals a fine, almost columnar, grain structure. Comparison of these two microstructures reveals that substitution of lanthanum with praseodymium results in a marked change in the grain structure of the cast alloys.

These alloys are mainly composed of the matrix phase and other secondary phases at the grain boundaries. The chemical compositions of the matrix phases in the different alloys, as determined by EDX, are presented in Table 2. The chemical composition of the other phases is discussed later. As expected, praseodymium substitutes lanthanum in the matrix phase of all the alloys. In general, in these alloys, good agreement has been found among the various measurements. The rare

Table 1. Composition of the as-cast $La_{0.7-x}Pr_xMg_{0.3}Al_{0.3}Mn_{0.4}Co_{0.5}Ni_{3.8}$ alloys.

Nominal composition and Substitution composition (at.%)	x	Specified and analyzed composition wt. (%)							
		La	Pr	Mg	Al	Mn	Co	Ni	C*
$La_{0.7}Mg_{0.3}Al_{0.3}Mn_{0.4}Co_{0.5}Ni_{3.8}$	0.0	25.12	-	1.88	2.09	5.68	7.61	57.62	-
$La_{11.67}Mg_5Al_5Mn_{6.67}Co_{8.33}Ni_{63.33}$	0.0	24.57	-	1.62	1.90	5.58	7.67	58.55	62
$La_{0.6}Pr_{0.1}Mg_{0.3}Al_{0.3}Mn_{0.4}Co_{0.5}Ni_{3.8}$	0.1	21.52	3.64	1.88	2.09	5.67	7.61	57.59	-
$La_{10}Pr_{1.67}Mg_5Al_5Mn_{6.67}Co_{8.33}Ni_{63.33}$	0.1	21.01	3.88	1.71	2.03	5.57	7.77	57.93	94
$La_{0.4}Pr_{0.3}Mg_{0.3}Al_{0.3}Mn_{0.4}Co_{0.5}Ni_{3.8}$	0.3	14.33	10.90	1.88	2.09	5.67	7.60	57.53	-
$La_{6.67}Pr_5Mg_5Al_5Mn_{6.67}Co_{8.33}Ni_{63.33}$	0.3	13.63	10.90	1.77	2.06	5.55	7.72	58.28	97
$La_{0.2}Pr_{0.5}Mg_{0.3}Al_{0.3}Mn_{0.4}Co_{0.5}Ni_{3.8}$	0.5	7.16	18.15	1.88	2.09	5.66	7.59	57.47	-
$La_{3.34}Pr_{8.33}Mg_5Al_5Mn_{6.67}Co_{8.33}Ni_{63.33}$	0.5	6.82	18.18	1.70	2.00	5.63	7.64	57.93	73
$Pr_{0.7}Mg_{0.3}Al_{0.3}Mn_{0.4}Co_{0.5}Ni_{3.8}$	0.7	-	25.39	1.88	2.08	5.66	7.59	57.41	-
$Pr_{11.67}Mg_5Al_5Mn_{6.67}Co_{8.33}Ni_{63.33}$	0.7	-	23.98	1.54	2.12	5.62	7.92	58.73	90

*ppm (impurity).

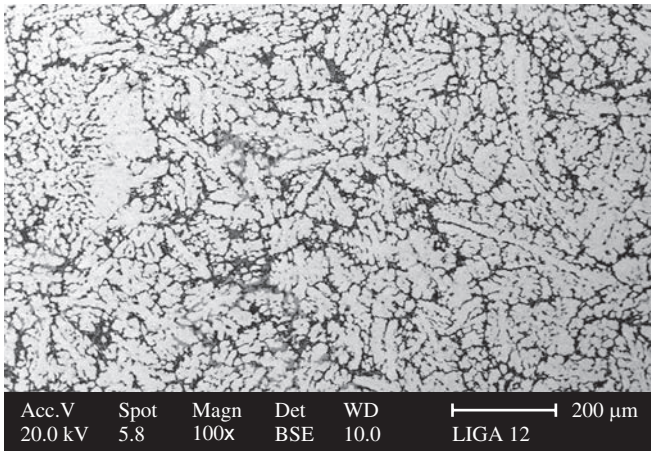

Figure 1. Backscattered electron image of the as-cast microstructure of the $La_{0.7}Mg_{0.3}Al_{0.3}Mn_{0.4}Co_{0.5}Ni_{3.8}$ alloy.

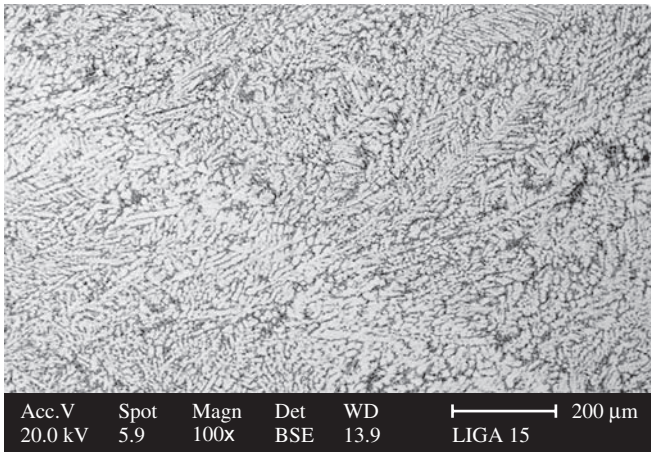

Figure 2. Backscattered electron image of the as-cast microstructure of the $Pr_{0.7}Mg_{0.3}Al_{0.3}Mn_{0.4}Co_{0.5}Ni_{3.8}$ alloy.

Table 2. Composition determined by EDX at the centers of the matrix phase, the major phase in the $La_{0.7-x}Pr_xMg_{0.3}Al_{0.3}Mn_{0.4}Co_{0.5}Ni_{3.8}$ alloys.

x	Analyzed composition (at.%)							N*
	La	Pr	Mg	Al	Mn	Co	Ni	
0.0	15.4 ± 0.6	-	<1	3.6 ± 0.3	3.6 ± 0.6	8.3 ± 0.5	68.4 ± 1.2	5
0.1	13.1 ± 0.3	2.5 ± 0.2	<1	4.2 ± 0.5	3.4 ± 0.8	8.2 ± 0.3	68.0 ± 0.1	9
0.3	8.5 ± 0.1	7.0 ± 0.4	<1	4.2 ± 0.6	3.1 ± 0.9	8.2 ± 0.4	68.0 ± 1.5	11
0.5	4.1 ± 0.1	11.1 ± 0.6	<1	4.4 ± 0.6	3.7 ± 0.9	8.4 ± 0.3	67.6 ± 1.1	11
0.7	-	14.8 ± 0.9	1.1 ± 0.7	4.2 ± 0.7	3.5 ± 1.2	8.3 ± 0.5	68.0 ± 1.4	17

*number of independent measurements from the matrix phase.

earth (RE) content in the matrix phase of all the alloys was about 15 at.%. The magnesium content in these alloys was below the detection limit of EDX (assumed as 1 at.%). Aluminium, manganese and cobalt were detected inside the matrix phase of all the alloys.

The matrix phase of all the alloys revealed a RE: (Al, Mn, Co, Ni) atomic ratio of approximately 5, indicating it to be a 1:5-type phase. Hence, in the matrix phase of these $LaNi_5$-type alloys, Mg was not detected (Mg-free phase), La was substituted by Pr and Ni was replaced by Al, Mn and Co.

Figure 3 shows a backscattered electron micrograph of the $La_{0.4}Pr_{0.3}Mg_{0.3}Al_{0.3}Mn_{0.4}Co_{0.5}Ni_{3.8}$ alloy in the as-cast state. In this micrograph a mixture of the two microstructures, mentioned earlier, is seen and the grain boundaries are well defined. Details of the grain boundaries in this alloy are shown in Figure 4. Three phases can be readily observed, namely: a grey phase (G), a dark phase (D) and the matrix phase (M).

The chemical composition of the grey phase in all the alloys, determined using EDX, is shown in Table 3. Once again, in all the

alloys, lanthanum was substituted by praseodymium in this phase and the measured value of rare earth (8.2~9.1 at.%) was approximately half of that found in the matrix phase (14.8~15.6 at.%). The aluminium content in the grey phase (~3 at.%) was lower, but still close to that found in the matrix phase (~4 at.%). Conversely, the magnesium content in this phase was as high as 11 at.%, whereas in the matrix phase, below the detection limit of EDX. The manganese content (7~9 at.%) in the grey phase was twice as much as that measured in the matrix phase (2.5~3.6 at.%). In all the alloys, the grey phase revealed a (RE,Mg):(Al, Mn, Co, Ni) atomic ratio of about 4, indicating a possible $PrMgNi_4$-type phase[12] or $LaMgNi_4$-type phase[13,14], even though the RE:Mg atomic ratio varied from 0.75 to 0.9.

The chemical composition of the dark phase in the different alloys, as determined using EDX, is presented in Table 4. The lanthanum-content was close or below the EDX detection limit. Conversely, Pr could not be detected or was below the detection limit for the alloy with $x < 0.3$. However, the Pr content of alloys with x equal to 0.5 and 0.7 could be determined.

EDX analyses also showed that the dark phase was very heterogeneous, and the content of the main elements (Mg, Al, Mn, Co, Ni) varied considerably. This can be attributed to the as-cast condition of these alloys. This is consistent with previous studies[15,16], where it was shown that in a $La_{0.7}Mg_{0.3}Al_{0.2}Mn_{0.1}Co_{0.75}Ni_{2.45}$ alloy, annealing at high temperature was essential to achieve a homogeneous composition. XRD and Rietveld analyses revealed that the major phases in all al-

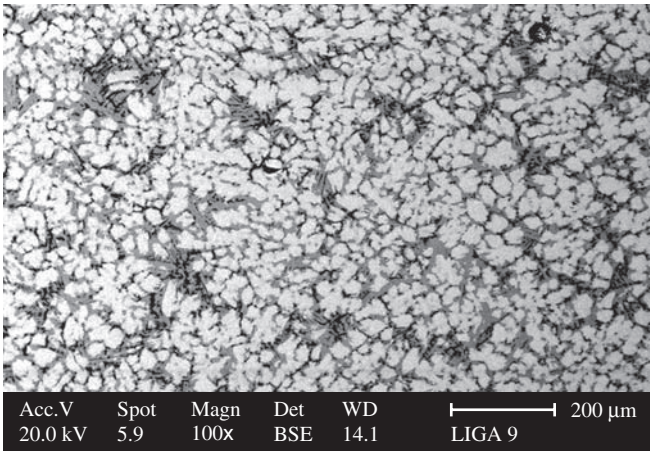

Figure 3. Backscattered electron image showing a general view of the as-cast microstructure of the $La_{0.4}Pr_{0.3}Mg_{0.3}Al_{0.3}Mn_{0.4}Co_{0.5}Ni_{3.8}$ alloy.

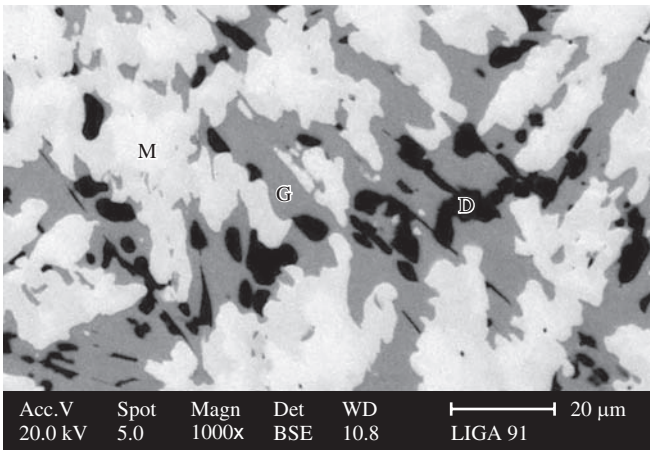

Figure 4. Backscattered electron image of details of the microstructure of the $La_{0.4}Pr_{0.3}Mg_{0.3}Al_{0.3}Mn_{0.4}Co_{0.5}Ni_{3.8}$ alloy.

Table 3. Composition determined using EDX at the centers of the grey phase in the as-cast $La_{0.7-x}Pr_xMg_{0.3}Al_{0.3}Mn_{0.4}Co_{0.5}Ni_{3.8}$ alloys.

x	Analyzed composition (at.%)							N
	La	Pr	Mg	Al	Mn	Co	Ni	
0.0	8.2 ± 0.3	-	10.9 ± 0.2	2.9 ± 0.4	9.5 ± 1.8	7.6 ± 0.1	60.9 ± 1.7	2
0.1	7.3 ± 0.6	1.2 ± 0.2	11.5 ± 0.2	3.1 ± 0.3	8.8 ± 0.8	8.3 ± 0.3	59.8 ± 0.8	2
0.3	5.0 ± 0.3	4.3 ± 0.2	12.0 ± 0.6	3.7 ± 0.1	6.5 ± 0.5	7.4 ± 0.2	61.0 ± 0.3	7
0.5	2.6 ± 0.2	6.4 ± 0.4	11.2 ± 0.3	3.0 ± 0.5	7.6 ± 0.9	8.1 ± 0.3	61.1 ± 0.9	5
0.7	-	9.1 ± 1.2	10.1 ± 0.1	3.4 ± 0.4	7.3 ± 1.2	7.6 ± 0.9	62.5 ± 0.6	2

Table 4. Composition determined using EDX at the centers of the dark phase in the as-cast $La_{0.7-x}Pr_xMg_{0.3}Al_{0.3}Mn_{0.4}Co_{0.5}Ni_{3.8}$ alloys.

x	Analyzed composition (at.%)							N
	La	Pr	Mg	Al	Mn	Co	Ni	
0.0	<1	-	1.8 ± 0.2	9.5 ± 0.4	15.1 ± 0.1	16.2 ± 0.3	56.8 ± 0.2	3
0.1	<1	<1	1.3 ± 0.1	9.6 ± 0.3	15.5 ± 0.1	16.7 ± 0.5	56.0 ± 0.5	2
	1.4 ± 0.3	<1	1.8 ± 0.2	16.7 ± 0.3	19.5 ± 0.1	8.3 ± 0.1	52.1 ± 0.2	3
	<1	<1	3.5 ± 0.4	18.6 ± 1.3	17.3 ± 2.1	8.8 ± 0.4	50.9 ± 0.9	8
	2.4 ± 0.2	<1	3.9 ± 0.9	11.7 ± 2.2	14.9 ± 1.7	11.1 ± 0.6	55.4 ± 1.1	2
0.3	<1	<1	<1	10.3 ± 0.3	15.5 ± 0.6	15.7 ± 0.4	56.3 ± 0.9	6
0.5	<1	<1	<1	16.6 ± 0.1	19.9 ± 1.3	8.9 ± 0.3	52.5 ± 0.2	2
	<1	1.6 ± 1.5	3.4 ± 0.1	15.2 ± 1.4	19.0 ± 3.1	8.4 ± 0.6	51.6 ± 1.8	2
	3.2 ± 0.4	7.5 ± 0.1	8.1 ± 0.4	4.1 ± 1.4	8.3 ± 0.4	8.4 ± 0.1	60.4 ± 0.1	2
0.7	-	1.8 ± 0.6	-	9.5 ± 0.7	16.1 ± 0.3	13.6 ± 0.2	59.1 ± 0.1	2
	-	6.2 ± 1.7	7.3 ± 0.9	5.6 ± 1.6	10.1 ± 1.3	9.4 ± 0.9	61.4 ± 0.9	2

loys were the (La,Mg)Ni_3 phase and the $LaNi_5$ phase. These studies also reported that the discharge capacity and cycle life improved upon annealing the alloy, but the electrochemical kinetics of the electrodes deteriorated after this treatment[15].

Heat treatment of the alloys mentioned in this investigation are being carried out assuming that the composition is similar to that studied previously[15]. It is very likely that the grey and the dark phases will form the (La,Mg)Ni_3 phase. Annealing (high vacuum and temperature) increases the production cost of the electrode. Hence, this heat treatment should be used only if the discharge capacity increase is worth the increase in processing cost. In the as-cast condition, the $La_{0.7}Mg_{0.3}Al_{0.2}Mn_{0.1}Co_{0.75}Ni_{2.45}$ alloy showed a maximum discharge capacity of 350.9 mAh.g^{-1} and this value increased to only to 370.0 mAh.g^{-1} with heat treatment at 1173 K for 8 hours[15].

Figures 5 and 6 show the X ray diffraction spectra of the as-cast La-Pr-based alloys for *x* equal to 0 and 0.1, respectively. Four phases were identified in the powder sample of $La_{0.7}Mg_{0.3}Al_{0.3}Mn_{0.4}Co_{0.5}Ni_{3.8}$ alloy: La(Ni,Co)$_5$ (SG: P6/mmm– PDF: 50-0777), LaAl(Ni,Co)$_4$ (SG: P6/mmm-PDF: 51-0893), La_2(Ni,Co)$_7$ (SG: P63/mmc–PDF: 22-0640) and AlMn(Ni,Co)$_2$ (SG: Fm3m–PDF: 40-1207).

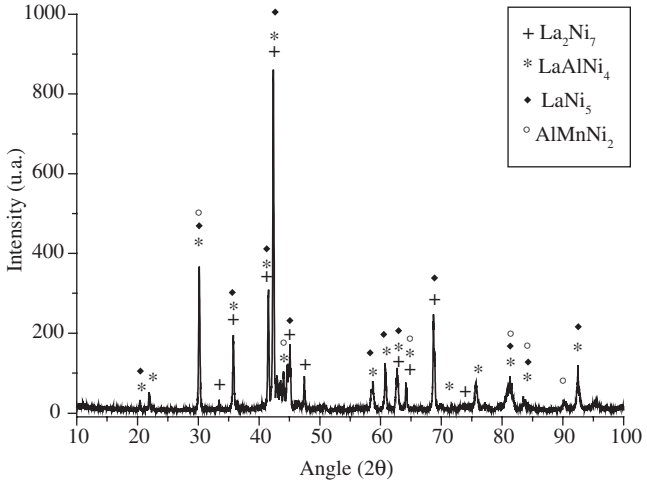

Figure 5. X ray diffraction spectrum of the $La_{0.7}Mg_{0.3}Al_{0.3}Mn_{0.4}Co_{0.5}Ni_{3.8}$ alloy.

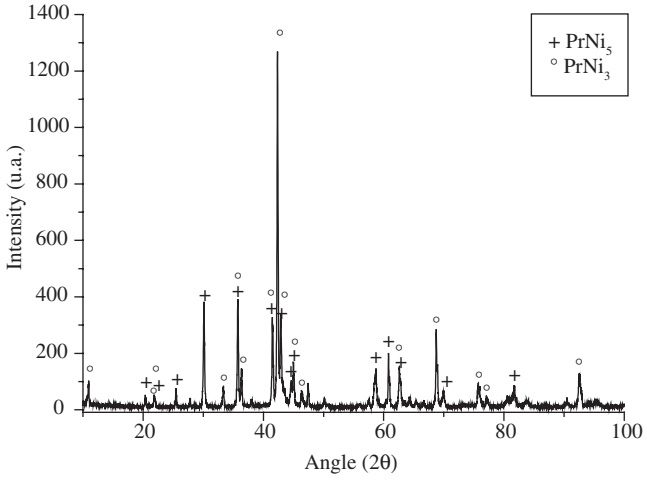

Figure 6. X ray diffraction spectrum of the $La_{0.6}Pr_{0.1}Mg_{0.3}Al_{0.3}Mn_{0.4}Co_{0.5}Ni_{3.8}$ alloy.

The differences in the observed reflections positions to the standards could be attributed to the phase substitutions of Mg, Mn and Co, present in the alloys. The presence of praseodymium in the alloys favors the formation of a phase with rhombohedral $PuNi_3$-type structure (SG: R-3m–PDF: 41-1129), as reported previously[15]. This can be observed in the XDR spectrum of $La_{0.6}Pr_{0.1}Mg_{0.3}Al_{0.3}Mn_{0.4}Co_{0.5}Ni_{3.8}$ alloy in Figure 6, and also in the spectra of other Pr-containing alloys. The site occupied by Pu in the $PuNi_3$-type structure is probably occupied by Pr, La and Mg. These phases are present alongside the La(Ni,Co)$_5$ and LaAl(Ni,Co)$_4$ phases. The doublet situated at 2θ = 36° in Figure 6 (also observed for $x = 0.3$, 0.5 and 0.7) indicates substitution of La with Pr in the crystalline $PuNi_3$-type structure (further refinement is necessary to confirm this). The XDR spectra for the Pr-containing alloys showed the $PrNi_5$ phase also (SG: P6/mmm–PDF: 12-0502). It is worthwhile noting that Co substitutes Ni in the structures, yielding phases of the type: Pr(Ni,Co)$_5$ and Pr(Ni, Co)$_3$. The La or $PrMgNi_4$-type phases could not be identified in the XDR spectra of the alloys that were studied. Determination of the structure of $AMgNi_4$ alloys (where A = Ca, La, Ce, Pr, Nd and Y) have been done by Guinier-Hägg X ray powder diffraction[17]. The compounds have a cubic $SnMgCu_4$ ($AuBe_5$-type) structure, which is related to the $(C_{15})MgCu_2$ structure.

Figure 7 shows the Pr-concentration vs. the *d*-spacings for the maximum intensity peak observed in the XDR spectra of the alloys.

The substitution of La with Pr shifts the maximum intensity peak position and consequently the cell volume (d_{hkl} varied from 2.1111 Å to 2.1329 Å, for $x = 0.7$ and 0, respectively). Cell volume and its variations play an important role in the performance of the electrode alloy. It has been reported that after Ni was partially substituted with Al, the cell volume expansion ratio of the La-Mg-Ni-based alloy decreased upon hydrogenation and pulverization of the alloy was inhibited, with consequent improvement in cycling stability of the electrode[18].

4. Conclusions

Substitution of La with Pr in the LaMgAlMnCoNi-based alloys changed the grain structure from equiaxial to columnar. The relative atomic ratio RE:(Al, Mn, Co, Ni), used as an indicator of the matrix phase, was 1:5 for the $La_{0.7-x}Pr_xMg_{0.3}Al_{0.3}Mn_{0.4}Co_{0.5}Ni_{3.8}$ alloys, as determined by energy-dispersive X ray spectrometry. Clearly, in spite of alloying element substitution, the matrix phase remained as

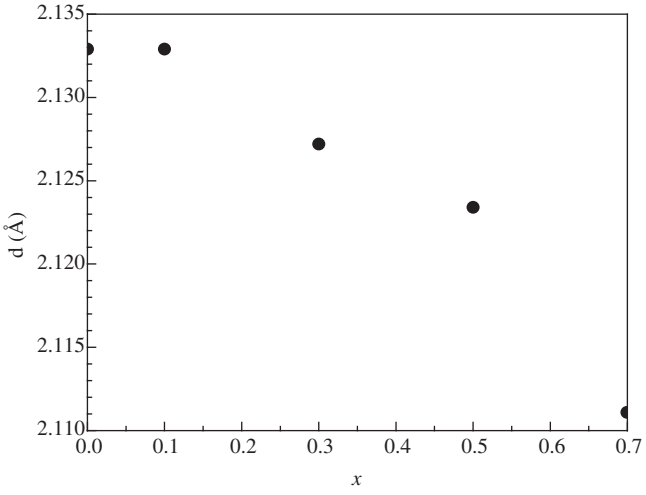

Figure 7. Praseodymium concentration (*x*) vs. the *d*-values for I/I_o=100 for the as-cast $La_{0.7-x}Pr_xMg_{0.3}Al_{0.3}Mn_{0.4}Co_{0.5}Ni_{3.8}$ alloys ($x = 0$, 0.1, 0.3, 0.5 and 0.7).

$LaNi_5$-type in these hydrogen storage alloys. Magnesium was only detected in the other two phases of these alloys. A grey phase revealed 11 at.% of Mg and the EDX ratio of concentration gave a composition close to the $PrMgNi_4$ phase. The dark phase, also detected using EDX, proved to be very heterogeneous in composition, and this was attributed to the as-cast state of these alloys. XRD spectra showed a shift in the *d*-spacing with increasing praseodymium content in the cast alloys. XRD analyses helped identify four phases in the $La_{0.7}Mg_{0.3}Al_{0.3}Mn_{0.4}Co_{0.5}Ni_{3.8}$ alloy, namely: $La(Ni,Co)_5$, $LaAl(Ni,Co)_4$, $La_2(Ni,Co)_7$ and $AlMn(Ni,Co)_2$. The XRD spectra of the Pr-containing alloys showed the phases $La(Ni,Co)_5$ and $LaAl(Ni,Co)_4$, and also that Pr favored the formation of a phase with $PuNi_3$-type structure, where Pu is substituted by Pr, La and Mg. Cobalt, on the other hand, substituted nickel in the structures and yielded phases of the type: $Pr(Ni,Co)_5$ and $Pr(Ni, Co)_3$.

Acknowledgments

The authors wish to thank FAPESP and IPEN-CNEN/SP for the financial support and infrastructure made available to carry out this investigation. Thanks are also due to C.V. Morais and G.A.F. Machado for help with the SEM analyses and also to R.R. Oliveira for technical assistance with the XDR analyses.

References

1. Lei Y, Jiang J, Sun D, Wu J, Wang Q. Effect of rare earth composition on the electrochemical properties of multicomponent $RENi_{5-x}M_x$ (M = Co, Mn, Ti) alloys. *Journal of Alloys and Compounds*. 1995; 231(1-2): 553-557.
2. Zhaoliang Z, Dongsheng S. Effects of particle size on the electrochemical properties of $Mm(NiCoMnAl)_5$ alloy. *Journal of Alloys and Compounds*. 1998; 270(1-2): L7-L9.
3. Willey DB, Harris IR, Pratt AS. The improvement of the hydrogenation properties of nickel-metal hydride battery alloy by surface modification with platinum group metals (PGMs). *Journal of Alloys and Compounds*. 1999 Dec 20; 293/295: 613-620.
4. Yeh MT, Beibutian VM, Hsu SE. Effect of Mo additive on hydrogen absorption of rare-earth based hydrogen storage alloy. *Journal of Alloys and Compounds*. 1999 Dec 20; 293/295: 721-723.
5. Jain IP, Abu Dakka MIS, Vijay YK. Hydrogen absorption in Al doped $MmNi_5$. *International Journal of Hydrogen Energy*. 2000; 25(7): 663-667.
6. Ye H, Xia B, Wu W, Du K, Zhang H. Effect of rare earth composition on the high-rate capability and low-temperature capacity of AB_5-type hydrogen storage alloys. *Journal of Power Sources*. 2002; 111(1): 145-151.
7. Willey DB, Pederzolli D, Pratt AS, Swift J, Walton A, Harris IR. Low temperature hydrogenation properties of platinum group metal treated, nickel metal hydride electrode alloy. *Journal of Alloys and Compounds*. 2002 Jan 17; 330/332: 806-809.
8. Yoshinaga H, Arami Y, Kajita O, Saka, T. Highly densed-MH electrode using flaky nickel powder and gas-atomized hydrogen storage alloy powder. *Journal of Alloys and Compounds*. 2002; 2002 Jan 17; 330/332: 846-850.
9. Latroche M, Chabre Y, Percheron Guegan A, Isnard O, Knosp B. Influence of stoichiometry and composition on the structural and electrochemical properties of AB_{5+y}-based alloys used as negative electrode materials in Ni-MH batteries. *Journal of Alloys and Compounds*. 2002 Jan 17; 330/332: 787-791.
10. Qingxue Z, Joubert JM, Latroche M, Jun D, Percheron Guegan A. Influence of the rare earth composition on the properties of Ni-MH electrodes. *Journal of Alloys and Compounds*. 2003; 360(1-2): 290-293.
11. Chen ZH, Lu MQ, Wang YL, Hu ZQ. Effect of Pr content in Ml on the electrochemical properties of $Ml(Ni-Co-Mn-Al)_5$ alloys. *Journal of Alloys and Compounds*. 1995; 231(1-2): 550-552.
12. Xu X, Zhou HY, Zou RP, Zhang SL, Wang ZM. Hydrogen storage properties of new ternary alloys: $PrMg_2Ni_9$ and $PrMgNi_4$. *Journal of Alloys and Compounds*. 2005; 396(1-2): 247-250.
13. Zhang F, Luo Y, Chen J, Yan R, Kang L, Chen J. Effect of annealing treatment on structure and electrochemical properties of $La_{0.67}Mg_{0.33}Ni_{2.5}Co_{0.5}$ alloy electrodes. *Journal of Power Sources*. 2005 Oct 4; 150: 247-254.
14. Wang ZM, Zhou HY, Gu ZF, Cheng G, Yu AB. Preparation of $LaMgNi_4$ alloy and its electrode properties. *Journal of Alloys and Compounds*. 2004; 377(1-2): L7-L9.
15. Pan H, Chen N, Gao M, Li R, Lei Y, Wang Q. Effects of annealing temperature on structure and the electrochemical properties of $La_{0.7}Mg_{0.3}Ni_{2.45}Co_{0.75}Mn_{0.1}Al_{0.2}$ hydrogen storage alloy. *Journal of Alloys and Compounds*. 2005; 397(1-2): 306-312.
16. Liu Y, Pan H, Li R, Lei Y. Effects of Al on cycling stability of a new rare-earth Mg-based hydrogen storage alloy. In: Zhong ZY, Saka H, Kim TH, Holm EA, Han YF, Xie XS, editors. *Proceedings of the Fifth Pacific Rim International Conference on Advanced Materials and Processing; 2004 Nov 2-5; Beijing, China.* Stafa-Zurich: Trans Tech Publications. *Materials Science Forum*. 2005; 475/479(Part 3): 2457-2462.
17. Kadir K, Noreus D, Yamashita I. Structural determination of $AMgNi_4$ (where A = Ca, La, Ce, Pr, Nd and Y) in the $AuBe_5$ type structure. *Journal of Alloys and Compounds*. 2002; 345(1-2): 140-143.
18. Sun X, Pan H, Gao M, Li R, Lin Y, Ma S. Cycling stability of La-Mg-Ni-Co type hydride electrode with Al. *Transactions of Nonferrous Metals Society of China*. 2006; 16(1): 8-12.